A Spatiotemporal Statistical Model for Eyeballs of Human Embryos

Masashi KISHIMOTO[†a)], **Atsushi SAITO**[†], **Tetsuya TAKAKUWA**[††], **Shigehito YAMADA**[††],
Hiroshi MATSUZOE[†††], *Nonmembers*, **Hidekata HONTANI**[†††], *Member*, **and** **Akinobu SHIMIZU**[†b)], *Fellow*

SUMMARY During the development of a human embryo, the position of eyes moves medially and caudally in the viscerocranium. A statistical model of this process can play an important role in embryology by facilitating qualitative analyses of change. This paper proposes an algorithm to construct a spatiotemporal statistical model for the eyeballs of a human embryo. The proposed modeling algorithm builds a statistical model of the spatial coordinates of the eyeballs independently for each Carnegie stage (CS) by using principal component analysis (PCA). In the process, a q-Gaussian distribution with a model selection scheme based on the Aaike information criterion is used to handle a non-Gaussian distribution with a small sample size. Subsequently, it seamlessly interpolates the statistical models of neighboring CSs, and we present 10 interpolation methods. We also propose an estimation algorithm for the CS using our spatiotemporal statistical model. A set of images of eyeballs in human embryos from the Kyoto Collection was used to train the model and assess its performance. The modeling results suggested that information geometry-based interpolation under the assumption of a q-Gaussian distribution is the best modeling method. The average error in CS estimation was 0.409. We proposed an algorithm to construct a spatiotemporal statistical model of the eyeballs of a human embryo and tested its performance using the Kyoto Collection.

key words: *computational anatomy, spatiotemporal model, embryo, Carnegie stage, growth*

1. Introduction

Statistical models of anatomical structures have played an important role in revealing variations of anatomical landmark points and surfaces. Many studies have shown the usefulness of medical image analysis techniques, such as segmentation and the assessment of the degree of abnormality by measuring deviation from a normal distribution [1]–[3]. Most such research has used data obtained through the observation of adults, whose anatomical structures can be assumed to be mature and homologous. While such data evinces statistical variation among subjects, there is no significant difference due to aging. However, when dealing with fetuses or infants, differences due to growth cannot be assumed to be negligible. To account for such changes, a spatiotemporal statistical model is required.

A number of spatiotemporal statistical models describe changes in time-varying features—growth in geometrical features, such as a point or a surface, and changes in the appearances of anatomical structures along a temporal axis [4]–[10]. Such models can be categorized according to the training data used to construct a spatiotemporal statistical model: namely, time-series data and longitudinal data [4]. Time-series data consists of a set of items indexed by any temporal marker, such as age, as an indicator of the given developmental stage. No assumption is made regarding whether a subset of the samples is observed from the same subject at different time points. In contrast, longitudinal data contains data repeatedly observed for same individual subjects.

This paper focuses on a spatiotemporal statistical model of the human embryo that can be useful for embryology in the qualitative analysis of change, where time-series data is available; that is, a time-indexed subject is observed once, and each data is from a different subject. Research on the construction of spatiotemporal statistical models from time-series data and longitudinal data [4]–[10] is as follows: the work in [4] involved constructing a spatiotemporal statistical model that can describe the evolution of the shape of longitudinal data, where the diffeomorphic deformation of the shapes was statistically modeled. It should be noted that a methodology for constructing a spatiotemporal statistical model that requires temporal change in the same subject cannot be applied to time-series data where no observation data is repeatedly available for the same subject. Only the work in [5] and [10] might be useful for our purpose here. Researchers in [5] constructed a cross-sectional atlas from time-series data and evaluated the correlation between the modes of variation and ages of the subjects. The work in [10] involved the construction of a model by simply assigning temporal weights to training data and constructing a spatiotemporal statistical model using weighted principal component analysis (PCA), which is a kind of cross-sectional approach with weights. A problem in these cross-sectional approach is the high complexity of the distribution to be analyzed. Although a number of non-linear statistical analysis methods [11], [12] have been proposed, PCA-based approaches play an important role in constructing statistical models due to their simplicity and robustness. In fact, both papers [5], [10] employed PCA. However, since PCA assumes a monomodal distribution, such as a Gaussian distribution, a cross-sectional approach to time-varying data

might render the distribution complex, hence degrading performance. A possible solution to this problem is to divide it into sub-problems, or to construct a model for each specific time and attempt to seamlessly concatenate the models constructed for different times.

This paper proposes an algorithm to construct a spatiotemporal statistical model for the location of the eyeballs in a human embryo using time-series data. The contributions of this study are as follows:

1. We propose an algorithm to construct a spatiotemporal statistical model with a continuous time parameter from time-series data, where a two-stage approach is employed. A statistical model for a specific time is constructed independently, and models for neighboring times are seamlessly interpolated. This approach is inspired by [13] and extended to a number of interpolation approaches in this paper.

2. We introduce q-Gaussian distribution-based parameter estimation [14] to spatiotemporal model construction. The approach allows the PCA-based approach to handle a non-Gaussian distribution with a small sample size.

3. A comparative study of 10 interpolation methods was carried out using images of human embryos from Carnegie stages (CSs) 17 to 23 of the Kyoto Collection [15]. Moreover, the effectiveness of the q-Gaussian distribution-based parameter estimation approach was verified. Note that the CS is a standardized staging system to supply a unified developmental chronology of the embryo [16]. The stages are decided according to the development of internal and external anatomical structures. The number of CS is originally an integer but extended to a continuous number in this study.

2. Method

In the developmental stages of a human embryo, the position of eyes moves medially and caudally in the viscerocranium [17]. The quantitative analysis of this growth is important in embryology. Our aim is to create a spatiotemporal model that describes this development in the context of the CS using time-series data from human embryos in the Kyoto Collection. Human embryos were scanned using a phase-contrast X-ray CT (PCX-CT) or a magnetic resonance imaging (MRI) scanner, and the centers of the eyeballs were identified by a human observer; they were used to construct the spatiotemporal statistical model. The input to the modeling process is a coordinate vector of the left and right eyeballs, the length of each of which is six following spatial standardization, where manually defined points on the first cervical vertebrae are aligned for all training cases. The proposed modeling algorithm is composed of two stages, i.e., modeling of each CS, and modeling intermediate neighboring CSs (Fig. 1).

In the first stage, coordinate vectors of the eyeballs of all embryos are mapped to a feature space spanned by eigenvectors, which are obtained as a result of PCA involving all CSs for efficient representation. Each CS is subsequently statistically modeled using PCA. Note that the number of eigenvectors is determined such that the ratio of their cumulative contribution is higher than 97%. The second stage involves modeling by interpolating intermediate models of neighboring CSs so that the model has a continuous time parameter and describes an eyeball location between CSs, such
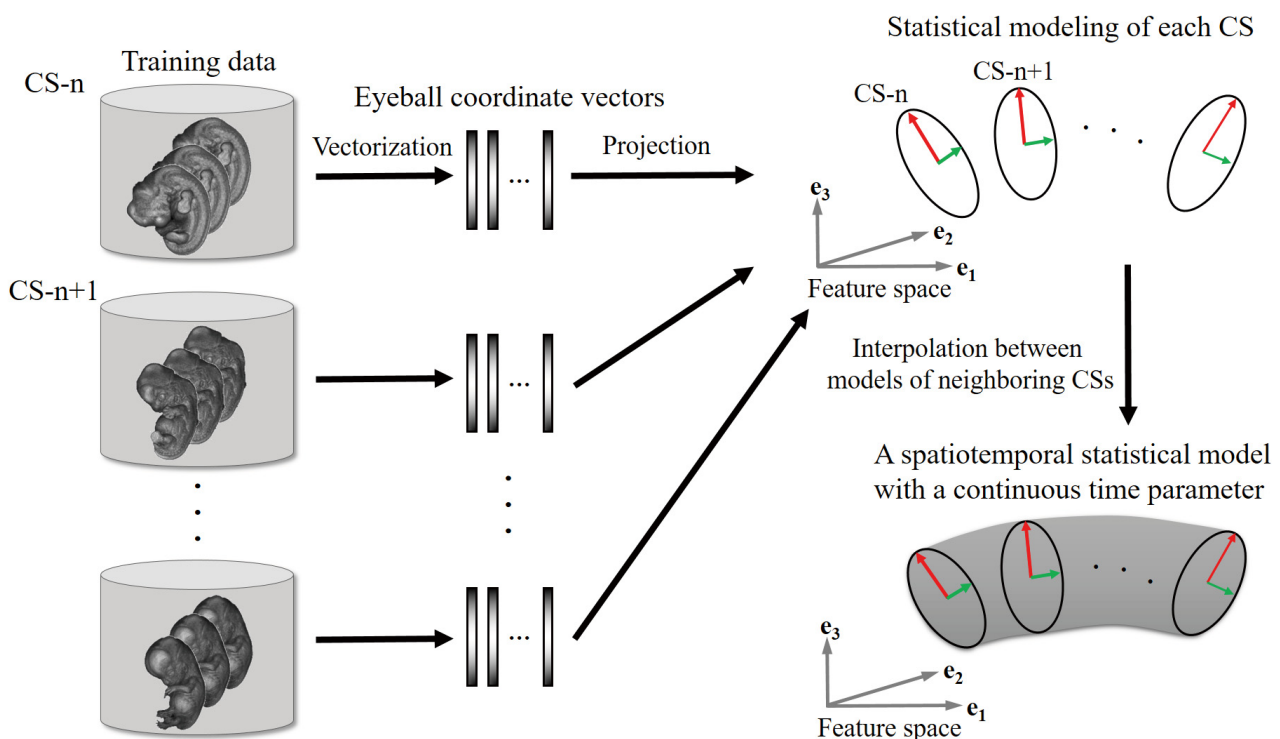

Fig. 1 Two-stage modeling approach for spatiotemporal statistical modeling

as location of CS18.4. A simple solution for interpolation is linear interpolation between neighboring average vectors as well as in terms of the rotation angle between neighboring covariance matrices [13]. We first present this simple modeling algorithm, and extend it in the subsequent subsection.

2.1 Spatiotemporal Modeling by Linear Interpolation

For simplicity of mathematical expression and without loss of generality, we present equations for interpolation between the covariance matrix of CS-0 and that of CS-1. Interpolations between CS-n and CS-n+1 (n = 17, . . . , 22) in the "Results" section can be easily derived from these equations.

Let the average vectors and covariance matrices of CS-0 and CS-1 be $\boldsymbol{\mu}_0$ and $\boldsymbol{\mu}_1$, and $\boldsymbol{\Sigma}_0$ and $\boldsymbol{\Sigma}_1$, respectively. Let $\mathbf{E}_0$ and $\mathbf{E}_1$ be matrices composed of the eigenvectors of $\boldsymbol{\Sigma}_0$ and $\boldsymbol{\Sigma}_1$. The average vector of CS-c ($0 \leqq c \leqq 1$) by linear interpolation can be described as follows:

$$\boldsymbol{\mu}_c = (1 - c)\boldsymbol{\mu}_0 + c\boldsymbol{\mu}_1 \tag{1}$$

The covariance matrix of CS-c ($0 \leqq c \leqq 1$) by rotation can be defined as follows:

$$\boldsymbol{\Sigma}_c = (\mathbf{U}\mathbf{D}(\boldsymbol{\varphi})^c\mathbf{U}^\dagger\mathbf{E}_0)\boldsymbol{\Lambda}_c(\mathbf{U}\mathbf{D}(\boldsymbol{\varphi})^c\mathbf{U}^\dagger\mathbf{E}_0)^T \tag{2}$$

where $\mathbf{U}$, $\mathbf{U}^\dagger$, and $\mathbf{D}(\boldsymbol{\varphi})^c$ represent a unitary matrix, its adjoint matrix, and a diagonal matrix generated by decomposing the rotation matrix $\mathbf{R}(\boldsymbol{\varphi})^c$ from $\mathbf{E}_0$ to $\mathbf{E}_1$, respectively. Vector $\boldsymbol{\varphi}$ is a rotation vector with dimension $\lfloor k/2 \rfloor$, where k is number of dimensions of the feature space. $\boldsymbol{\Lambda}_c$ is a diagonal matrix that consists of interpolated values between eigenvalues λ_{0j} of $\boldsymbol{\Sigma}_0$ and λ_{1j} ($j = 1, 2, \ldots, k$) of $\boldsymbol{\Sigma}_1$:

$$\lambda_{cj} = ((1 - c)\sqrt{\lambda_{0j}} + c\sqrt{\lambda_{1j}})^2 \tag{3}$$

The above covariance interpolation is ad hoc, and assumes that the nth eigenvector of CS-0 corresponds to the nth eigenvector of CS-1. However, such an assumption might not hold in our study. Thus, we employ four additional approaches to interpolation, Affine-invariant [18], Log-Euclidean [18], Wasserstein geometry [19], and information geometry [20], [21], none of which requires correspondence between eigenvectors.

Please note that it is not necessary for the proposed approaches to perform PCA in the statistical modeling of each CS. In that stage, they estimate an average vector and a covariance matrix of each CS in a feature space. These approaches, however, require PCA after the second stage to define axes of a spatiotemporal statistical model with a continuous time parameter.

2.2 Spatiotemporal Modeling without Correspondence between Eigenvectors

Affine-invariant Riemannian metrics were introduced to avoid defects in tensors due to Euclidean operations, and were successfully applied to diffusion tensor imaging [18].

The covariance matrix of CS-c ($0 \leqq c \leqq 1$) is interpolated along a standard geodesic on a manifold of positive-definite symmetric matrices and is given as follows:

$$\boldsymbol{\Sigma}_c = \boldsymbol{\Sigma}_0^{1/2} \exp\{c \log(\boldsymbol{\Sigma}_0^{-1/2}\boldsymbol{\Sigma}_1\boldsymbol{\Sigma}_0^{-1/2})\}\boldsymbol{\Sigma}_0^{1/2} \tag{4}$$

where the exp of any matrix $\mathbf{M}$ is defined by

$$\exp(\mathbf{M}) = \sum_{k=0}^{\infty} \frac{\mathbf{M}^k}{k!}$$

The matrix logarithm is given as the inverse of the exponential. Although the affine-invariant Riemannian metric exhibits excellent theoretical properties, its computational complexity is high. To address this limitation, a new family of Riemannian metrics called Log-Euclidean was proposed. It too shows excellent theoretical properties and similar results to Affine-invariant Riemannian metrics [18]. It is superior to the affine-invariant metric in terms of lower computational complexity. The covariance matrix of CS-c ($0 \leqq c \leqq 1$) by Log-Euclidean is presented as follows:

$$\boldsymbol{\Sigma}_c = \exp\{(1 - c)\log(\boldsymbol{\Sigma}_0) + c\log(\boldsymbol{\Sigma}_1)\} \tag{5}$$

Wasserstein geometry can derive a covariance matrix of CS-c ($0 \leqq c \leqq 1$) from the viewpoint of an optimal transport plan [19]. For Gaussian distributions, the covariance matrix of CS-c ($0 \leqq c \leqq 1$) is defined so that the transportation cost between two probability distributions is minimal:

$$\boldsymbol{\Sigma}_c = \{(1 - c)\mathbf{I} + c\mathbf{W}\}\boldsymbol{\Sigma}_0\{(1 - c)\mathbf{I} + c\mathbf{W}\} \tag{6}$$

where

$$\mathbf{W} = \boldsymbol{\Sigma}_1^{1/2}(\boldsymbol{\Sigma}_1^{1/2}\boldsymbol{\Sigma}_0\boldsymbol{\Sigma}_1^{1/2})^{-1/2}\boldsymbol{\Sigma}_1^{1/2} \tag{7}$$

Information geometry [20] is an alternative approach to defining the covariance matrix of CS-c ($0 \leqq c \leqq 1$) by linearly interpolating between the amounts of information of two probability distributions:

$$\boldsymbol{\Sigma}_c = \{(1 - c)\boldsymbol{\Sigma}_0^{-1} + c\boldsymbol{\Sigma}_1^{-1}\}^{-1} \tag{8}$$

Note that all of the above are interpolation methods involving two covariance matrices. Average interpolation is not defined except in information geometry, where it is given by the following equation [21]:

$$\boldsymbol{\mu}_c = \boldsymbol{\Sigma}_c\{(1 - c)\boldsymbol{\Sigma}_0^{-1}\boldsymbol{\mu}_0 + c\boldsymbol{\Sigma}_1^{-1}\boldsymbol{\mu}_1\}^{-1} \tag{9}$$

In this study, we compare all combinations between two average interpolation methods, or linear interpolation by Eq. (1) and information geometry-based interpolation by Eq. (9), and the five covariance matrix interpolation methods represented in Eqs. (2) and (4)-(6), (8). In total, 10 interpolation methods are compared in the "Result" section.

Above approaches do not require PCA in the statistical modeling of each CS, because they do not use correspondence between eigenvectors. However, it is necessary for the approaches to perform PCA after the second stage to
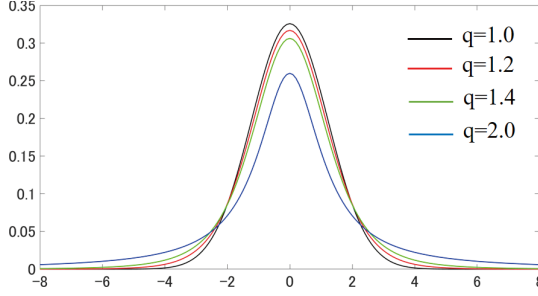
Fig. 2 q-Gaussian distribution with $\mu = 0$, $\Sigma = 1.5$

define axes of a spatiotemporal statistical model with a continuous time parameter.

2.3 q-Gaussian-Based Parameter Estimation

PCA assumes a monomodal distribution, such as a Gaussian distribution. PCA under the assumption of a Gaussian distribution works well for most cases. It does, however, sometimes fail in modeling due to the presence of an outlier and/or bias induced by overfitting to small datasets [22]. Furthermore, the distribution might be other than Gaussian, such as a student-t distribution, which is heavy tailed. To handle the above problem, we employ a q-Gaussian distribution-based approach [14] to estimate the average vector and the covariance matrix. The probability density function of a q-Gaussian distribution with average $\boldsymbol{\mu}$ and covariance $\boldsymbol{\Sigma}$ is as follows:

$$P_q(\mathbf{x}, \boldsymbol{\mu}, \boldsymbol{\Sigma}) \equiv Z[1 + \frac{1}{\nu}(\mathbf{x} - \boldsymbol{\mu})^T \boldsymbol{\Sigma}^{-1}(\mathbf{x} - \boldsymbol{\mu})]^{\frac{1}{1-q}} \qquad (10)$$

where

$$Z \equiv \frac{\Gamma(\frac{\nu+d}{2})}{(\pi\nu)^{\frac{d}{2}}\Gamma(\frac{\nu}{2})|\boldsymbol{\Sigma}|^{\frac{1}{2}}}$$

$$\nu = -d - \frac{2}{1-q}$$

The symbol d represents the dimensionality of space, and q must be smaller than $1 + \frac{2}{d}$ in order to satisfy the integrability of the probability density function. When parameter q is 1, it is a Gaussian distribution. When q is greater than 1, the distribution is heavy tailed, and closer to a student-t distribution (Fig. 2).

Due to the flexibility in the representation of the probability distribution, we expect that a q-Gaussian distribution-based approach might make the CS modeling process better than the conventional approach. However, it should be noted that the selection of parameter q, as well as the estimation of average $\boldsymbol{\mu}$ and covariance $\boldsymbol{\Sigma}$, are crucial to the success of the modeling process. In this study, we employ the Akaike information criterion (AIC) [23] to select parameter q, which is derived from a KL-divergence between the q-Gaussian distribution and the true one. Parameter q with minimum AIC is selected and used to build a spatiotemporal statistical model:

$$\text{AIC}(q) = -2\log L_q(\hat{\boldsymbol{\mu}}, \hat{\boldsymbol{\Sigma}}) + 2k \qquad (11)$$

where k is the number of parameters of the distribution and $L_q(\hat{\boldsymbol{\mu}}, \hat{\boldsymbol{\Sigma}})$ is the likelihood, with average and covariance estimated by the following EM algorithm with a fixed parameter q [24], where the initial values of the EM algorithm are given by a training dataset:

- E-STEP

$$w_i^{(m)} = \frac{\nu + d}{\nu + (\mathbf{x}^i - \boldsymbol{\mu}^{(m)})^T(\boldsymbol{\Sigma}^{(m)})^{-1}(\mathbf{x}^i - \boldsymbol{\mu}^{(m)})}$$

- M-STEP

$$\boldsymbol{\mu}^{(m+1)} = \frac{\sum_{i=1}^{M} w_i^{(m)} \mathbf{x}^i}{\sum_{i=1}^{M} w_i^{(m)}}$$

$$\boldsymbol{\Sigma}^{(m+1)} = \frac{1}{M} \sum_{i=1}^{M} w_i^{(m)}(\mathbf{x}^i - \boldsymbol{\mu}^{(m+1)})(\mathbf{x}^i - \boldsymbol{\mu}^{(m+1)})^T$$

Consequently, the algorithm to select the best q for a given dataset is shown below:

Algorithm 1 Optimization of q

Initialize; $q = 1$
while ($q < 1 + \frac{2}{d}$) **do**
    Estimate $\boldsymbol{\mu}$ and $\boldsymbol{\Sigma}$ by the EM algorithm given a fixed q
    Compute AIC(q)
    $q \Leftarrow q + \Delta q$
end while
Output; q^* with minimum AIC

To ensure that the selected value of q is better, we compute $L_q(\hat{\boldsymbol{\mu}}, \hat{\boldsymbol{\Sigma}})$ in a leave-one-out fashion. Note that the result of our study is consistent with the result when maximizing likelihood L_q, because k is constant. Finally, the average $\boldsymbol{\mu}$ and covariance $\boldsymbol{\Sigma}$ were estimated by the EM algorithm, with the optimized q using all the training data. The proposed q-Gaussian distribution-based approach is used not only to construct a feature space, but also to build a statistical model for each CS.

2.4   Carnegie Stage Estimation

An interesting application of the proposed spatiotemporal statistical model is to estimate the CS of a given test data. To this end, the Mahalanobis distance from the given data $\mathbf{x}$ to the average $\boldsymbol{\mu}_c$ ($0 \leqq c \leqq 1$) is calculated:

$$\sqrt{(\mathbf{x} - \boldsymbol{\mu}_c)^T \boldsymbol{\Sigma}_c^{-1}(\mathbf{x} - \boldsymbol{\mu}_c)} \qquad (12)$$

In the estimation process, c is sampled exhaustively between 0 to 1 with an interval of Δc. Subsequently, we find c with the minimum Mahalanobis distance and decide it as the estimated CS.

3. Results

3.1 Materials

This research was approved by Kyoto University's ethical review board. As shown in the top row of Fig. 3, we used time-series data from 180 human embryos in Carnegie stages 17 to 23 of the Kyoto Collection [15] which comprises approximately 44,000 human embryos. In most cases, pregnancy was terminated during the first trimester for socioeconomic reasons under the Maternity Protection Law of Japan. Some of the specimens (-20%) were undamaged, well-preserved embryos, from which 180 human embryos were randomly selected. Human embryos were scanned using a 2.35T MR system [25]. The 3D T1-weighted images were acquired using gradient echo sequence ($TR = 100ms, TE = 8ms$). The resolution of these images is $120\mu m^3$. The modeling target was the center of the lens of the eyeballs, or bilateral lens vesicles, as shown in the bottom row and was entered manually on the images by use of the Amira software (version 5.4.5; Visage Imaging, Berlin, Germany). Two people identified landmarks and there were no landmarks that were impossible to be identified. Figure 4 shows the landmarks on maxillofacial area. Please note that we used a volume rendering image to show landmarks instead of a cross-sectional image, because of better visibility.

Table 1 shows the number of samples for each CS, and Fig. 5 shows a bird's eye and frontal views of all data. The
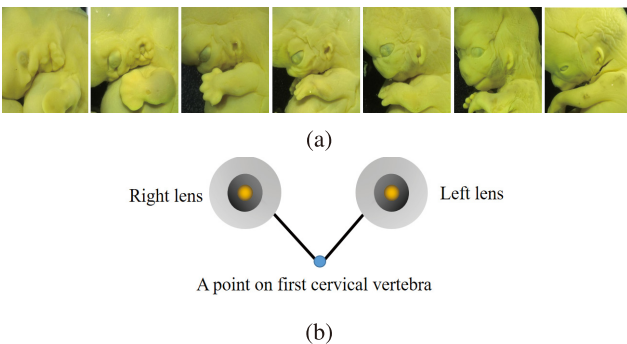

(a)

(b)

Fig. 3 Materials used to construct a spatiotemporal statistical model of the human embryo. (a) Examples of human embryos in Carnegie stages 17 to 23 of the Kyoto Collection. (b) Centers of lenses (yellow dots) that were the targets of modeling. Points of the first cervical vertebrae were aligned for all training data

Fig. 4 Left and right lens vesicle of the modeling target

figure confirms that both eyeballs develop toward the outside, symmetrically with respect to the median plane of the viscerocranium. In the statistical modeling process of these data, the numbers of eigenvectors of the first and second stages were three, their cumulative contribution ratios were greater than 97%. Interval Δc to estimate CS and Δq in Algorithm 1 were set to 0.01 in this study.

3.2 Spatiotemporal Model by Linear Interpolation

Figure 6 shows a spatiotemporal statistical model of the eyeballs obtained by linear interpolation, where the trajectories of the average ($\alpha = 0$) and the deviation along the first principal axis are highlighted using different colors.

3.3 Comparative Study of 10 Spatiotemporal Statistical Models

We first constructed 10 models under the assumption of a Gaussian distribution and compared them in terms of specificity [26], [27]. Note that there is another performance index called generalization that quantifies the ability of a

Table 1 Number of embryo-related data for each CS

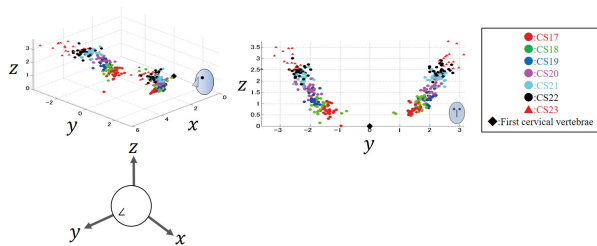| CS	17	18	19	20	21	22	23	sum
Sample #	30	27	21	28	30	26	18	180

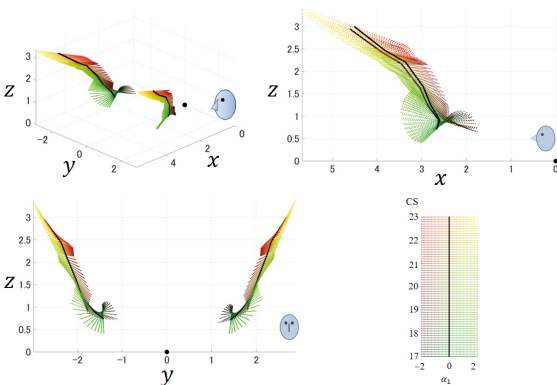**Fig. 5** Bird's eye and frontal views of all eyeballs

Fig. 6 Spatiotemporal statistical model of eyeballs in a human embryo during CS 17 to 23 constructed through linear interpolation under the assumption of a Gaussian distribution. This figure shows the trajectories of the average and the deviation along the 1st principal axis. The bottom right is a colored map displaying Carnegie stage "CS" and the 1st principal score "α_1".
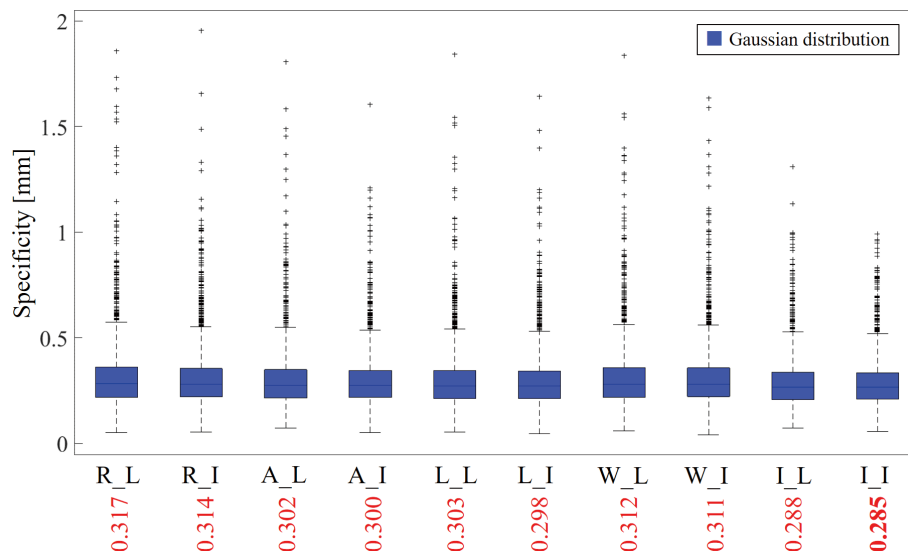
Fig. 7 Specificity of 10 interpolation methods where a Gaussian distribution was assumed. The combination of covariance-matrix interpolation (R: Rotation, A: Affine-invariant, L: Log-Euclidean, W: Wasserstein geometry, I: Information geometry) and average vector interpolation (L: Linear interpolation, I: Information geometry) is denoted by "Covariance_Average". Red numeral means "Specificity".
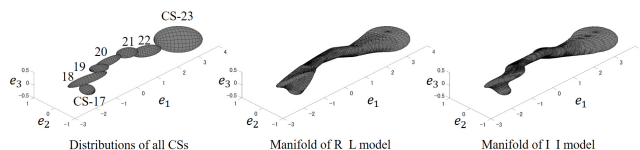

Fig. 8 Gaussian distributions of all CSs in a feature space, and manifolds of spatiotemporal statistical models by R_L and I_I (Iso-surface where the Mahalanobis distance from the average is 3). e_i represents i^{th} eigenvector.

model to describe instances not part of the training set. Generalization can be defined as an average of the reconstruction error between test data and back-projected data from the eigenshape space of a statistical model. However, all 10 models used a common feature space and eigenspace for each CS. Thus, the generalization was the same for all interpolation methods. Note that different interpolation methods generate different trajectories of the average and the eigenvectors in feature space, resulting in differences in specificity values, which reflect the ability to represent only valid instances of the object. In this study, we defined specificity as the average of the minimum reconstruction error between a test data item and 1,000 artificial data items generated by random numbers, the average and variance of which are identical to their counterparts values in a statistical model. Specificity was calculated by two-fold cross-validation.

Figure 7 shows boxplots of the specificities of the 10 models under the assumption of a Gaussian distribution. It can be seen from this figure that the information geometry-based approach yielded the best performance with respect not only to covariance interpolation, but also to average interpolation.

Figure 8 shows a Gaussian distributions of all CSs in a feature space and manifolds of models by R_L and I_I, re-

spectively. In this figure, we see that the interpolation due to I_I generated a model with low variance, whereas the R_L interpolation rendered greater the variance of earlier CSs. We assumed that lower variance would lead to higher specificity.

3.4 Comparative Study of q-Gaussian-Based Parameter Estimation

We constructed 10 models under the assumption of a q-Gaussian distribution, and compared them in terms of specificity. Figure 9 shows boxplots in terms of specificity. It can be confirmed from this figure that the information geometry-based approach yielded the best performance with respect not only to covariance interpolation, but also to average interpolation.

Figure 10 shows q-Gaussian distributions with optimized values of $q(= 1.23, 1.34, 1.16, 1.00, 1.19, 1.19, 1.29)$ for all CSs, where the optimized q in feature space was 1.17. The figures in the middle and to the right show manifolds of models by R_L and I_I, respectively. It should be noted that the distribution (left figure) of each CS have more compact support in comparison with Fig. 8, and the directions of the distributions are more aligned than those in Fig. 8, due to the superiority of q-Gaussian-based parameter estimation. The difference led to improvement in specificity from Fig. 7 to Fig. 9. Moreover, the manifolds of the right part (I_I) in Fig. 10 seemed to explain the transition between CSs appropriately, whereas the manifold of the middle figure (R_L) is piecewise linear, and seemed to fail to present the details of the transition between the CSs, resulting in lower specificity.

Figure 11 shows a spatiotemporal statistical model by I_I under the assumption of q-Gaussian distribution. The figure indicates that the variance in the location of the eyeballs
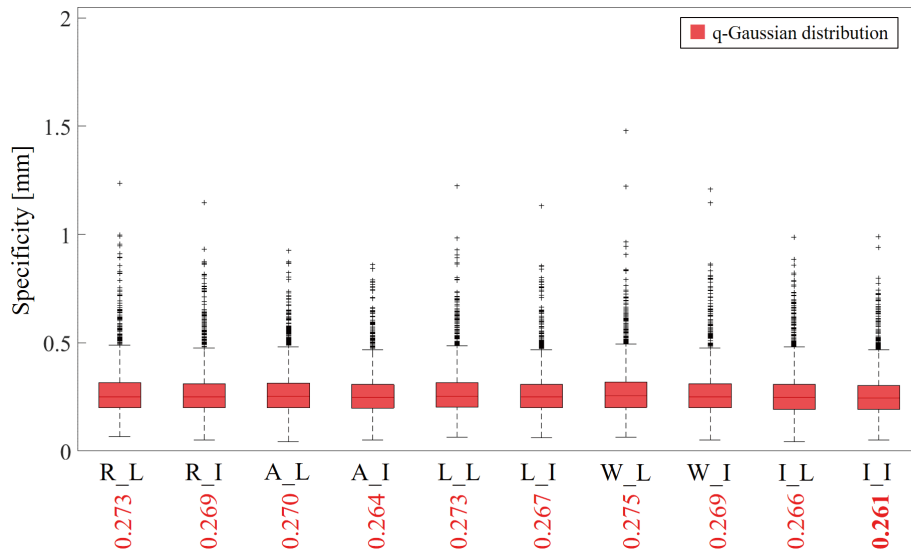
Fig. 9 Specificity of 10 interpolation methods under assumption of a *q*-Gaussian distribution with optimized parameter *q*. Combinations of covariance matrix interpolation (R: Rotation, A: Affine-invariant, L: Log-Euclidean, W: Wasserstein geometry, I: Information geometry) and average vector interpolation (L: Linear interpolation, I: Information geometry) are denoted by "Covariance_Average" in the figure. Red numeral means "Specificity".
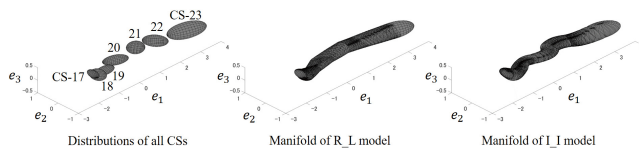

Fig. 10 *q*-Gaussian distributions of all CSs in a feature space, and manifolds of spatiotemporal statistical models by R_L and I_I (Iso-surface where the Mahalanobis distance from average = 3). e_i represents i^{th} eigenvector.
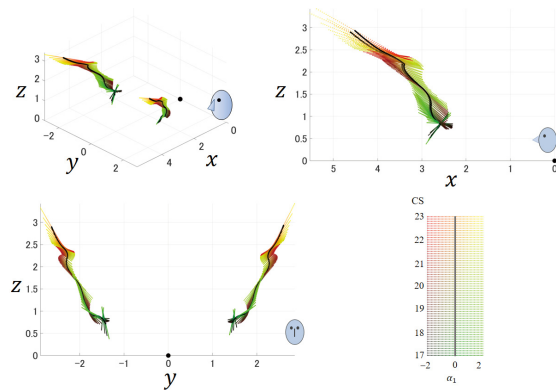

Fig. 11 Spatiotemporal statistical model of eyeballs in a human embryo in CS 17 to 23 constructed by I_I (average and covariance were interpolated by information geometry) under the assumption of a *q*-Gaussian distribution. These figures show the trajectories of the average and the deviation along the 1st principal axis. The bottom right is a colored map displaying Carnegie stage "CS" and the 1st principal score "α_1".

was smaller than that in Fig. 6 because the length of the segments proportional to the standard deviation along the 1st eigenvector became shorter.
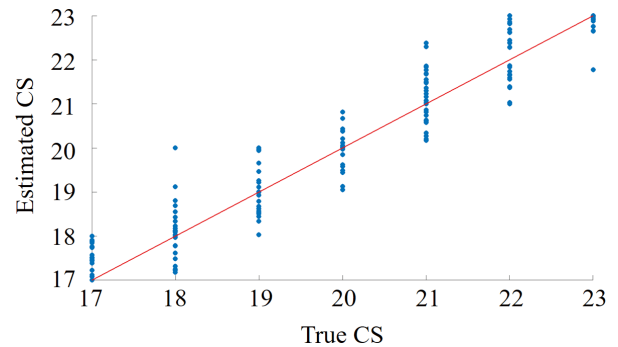

Fig. 12 Relationship between true CS and estimated CS in the best spatiotemporal model

3.5 Carnegie Stage Estimation

The CSs were estimated in a leave-one-out manner. We constructed a spatiotemporal statistical model, or the best one by information geometry (I_I), under the assumption of a *q*-Gaussian distribution by using the training dataset except for a test data. Then we applied the CS estimation algorithm with the model to the test data. We repeated this estimation process by changing the test data. Figure 12 shows the relationship between the true CS and the estimated CS, where the average error in the proposed estimation algorithm was 0.409.

4. Discussion

This paper proposed an algorithm to build a spatiotemporal statistical model of the eyeballs with a continuous time parameter by using time-series data from embryos, and pre-

sented a comparative study of 10 interpolation schemes. We confirmed that the information geometry-based approach under the assumption of a q-Gaussian distribution is the most suited to statistically modeling the spatiotemporal development of the eyeballs. The symmetrical growth of the right and left eyeballs in Fig. 5 seems to be efficiently and accurately modeled in Fig. 11.

To confirm the superiority of the information geometry-based approach over the linear interpolation-based approach in terms of specificity, we subjected the models to the Mann-Whitney U-test by R_L (interpolation by rotation for covariance matrix and linear interpolation for the average) and I_I (covariance and average were interpolated by information geometry) under the assumption of a q-Gaussian distribution. The null hypothesis H0 was that the distributions of specificity of the two approaches is identical. The p-value was 0.010, and H0 was rejected ($p < 0.05$). The superiority of information geometry might be explained by appealing to the fact that information geometry-based approaches interpolate between two distributions along the direction in which the Kullback-Leibler divergence between two points decreases maximally. The fact might derive more appropriate manifolds between two probabilistic distributions and bring the superiority demonstrated in the experiment. Further study using large dataset is required to confirm it in the future.

We also evaluated the difference between the Gaussian assumption and the q-Gaussian assumption in detail, when using the information geometry-based approach. We conducted statistical tests of the performance index between two assumptions (H0: the two distributions of the performance index are identical). For detailed comparisons, we calculated not only specificity, but also generalization as performance index. Note that q-Gaussian-based parameter estimation was adopted for feature space construction, where the number of dimensions of a given input vector was reduced from six to three. The Gaussian approach and the q-Gaussian-based approach derived different sets of eigenvectors, the directions of which were different from one another. Even though the number of dimension was identical, or three, for both approaches, the eigenspace spanned by the eigenvectors was different. This is why generalization was measured and compared between the Gaussian and the q-Gaussian-based approaches. Figure 13 shows a comparison between the Gaussian and the q-Gaussian-based approaches in terms of generalization (Wilcoxon signed-rank test) and specificity (Mann-Whitney U-test). Recall that both performance indices evaluated reconstruction error, where a smaller error is better. The figure tells us that the q-Gaussian-based approach is superior to the Gaussian based one in terms of statistically significant difference.

We also discuss the estimation error. The average estimation error of 0.409 was achieved using information geometry-based interpolation. We compared the errors in information geometry-based approach under the assumption of a q-Gaussian distribution with those under that of a Gaussian distribution (Fig. 14). Although the difference
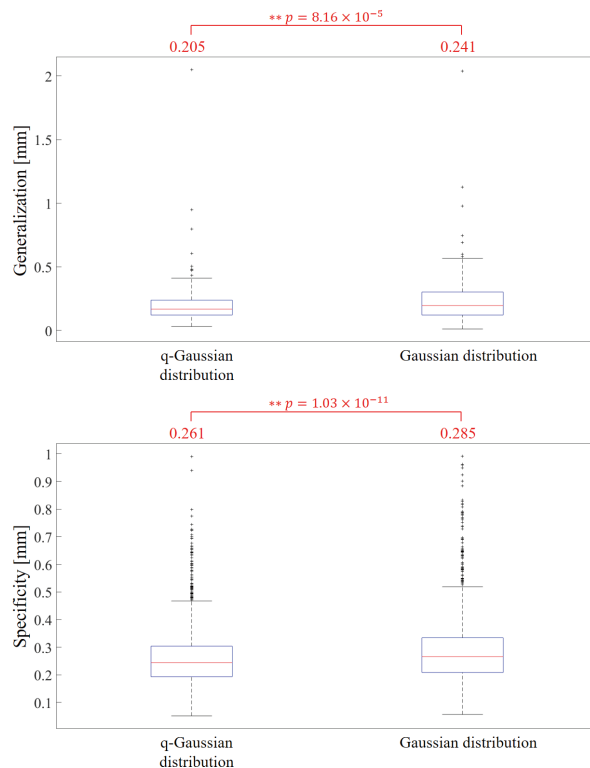

Fig. 13 Generalization and specificity of the information geometry-based model under assumptions of a q-Gaussian distribution and a Gaussian distribution
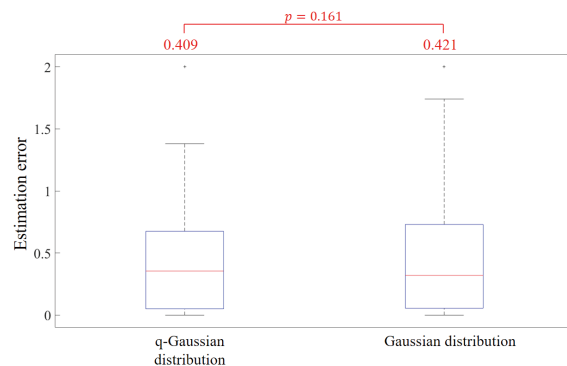

Fig. 14 Estimation error in the information geometry approach under assumptions of a q-Gaussian distribution and a Gaussian distribution

was not statistically significant (by the Wilcoxon signed-rank test), the q-Gaussian-based approach yielded slightly better performance. The results suggested that a q-Gaussian distribution-based approach might be found to be statistically effective in terms of CS estimation when the size of data for statistical test increases.

The average error might not be small enough to qualitatively analyze changes in embryology. One possible reason for the error is that the CS is a staging system that supplies a developmental chronology, and is mainly determined by the morphological development of the external appearance of the body of the embryo [16]. Since the location of the eyeballs is not considered in determining the CS of an embryo,

there occur overlaps in data between neighboring CSs, as shown in Fig. 5. Such overlaps give rise to inevitable error in CS estimation. Another possible reason is due to the quantization error in the staging process by a human observer, which is also difficult to solve. Although there are a number of difficulties in estimating the CS, it is be useful for qualitatively analyzing the changes in studies in embryology. For future work, we plan to improve estimation performance.

This paper focused on the eyeballs of embryos in a certain range of the CS. There are, however, a number of anatomically important landmarks of an embryo that need to be modeled. We plan to model the development of the eyeballs as well as the ears, and other important anatomical landmarks of the embryo. An extension of the proposed approach to modeling the surfaces of embryonic organs is another interesting task for future research. Furthermore, an algorithm for abnormal detection is an important application of the spatiotemporal model, and we plan to develop it for computer-aided diagnosis of embryos. For example, once we have a set of landmarks of a given embryo obtained through a non-invasive imaging scanner, we can estimate the deviation from the average using the proposed spatiotemporal model. When the deviation is large, we would say that the given subject is abnormal, and vice versa. Finally, an extension of the modelling algorithm is important. For example, we assumed that numbers of dimensions of neighboring CSs are same and our experiments met the assumption. However, the assumption might not be true for different anatomical structures. To deal with changes in dimensionality between neighboring CSs, we have to extend our modeling approaches that remains as future work.

5. Conclusion

This paper proposed an algorithm to construct a spatiotemporal statistical model for the movement by growth of eyeballs in a human embryo. The algorithm consists of two stages: modeling in each CS, and interpolation between models of neighboring CSs. In the first stage, a q-Gaussian distribution was introduced to handle a non-Gaussian distribution with a small sample size. In the second stage, 10 combinations of interpolation between neighboring CS were presented; furthermore, an estimation algorithm for the CS of given test data was presented. The algorithm was applied to the Kyoto Collection of images of human embryos to build a spatiotemporal model of the eyeballs, and performance was evaluated in terms of specificity, generalization, and CS estimation error. The best model was yielded by information geometry-based interpolation under assumption of a q-Gaussian distribution.

Acknowledgments

References

[1] T. Heimann and H.-P. Meinzer, "Statistical shape models for 3D medical image segmentation: a review," Medical image analysis, vol.13, no.4, pp.543–563, Aug. 2009.

[2] T.F. Cootes, C.J. Taylor, D.H. Cooper, and J. Graham, "Active shape models-their training and application," Computer vision and image understanding, vol.61, no.1, pp.38–59, Jan. 1995.

[3] D. Cremers, M. Rousson, and R. Deriche, "A review of statistical approaches to level set segmentation: integrating color, texture, motion and shape," International journal of computer vision, vol.72, no.2, pp.195–215, April 2007.

[4] S. Durrleman, X. Pennec, A. Trouvé, J. Braga, G. Gerig, and N. Ayache, "Toward a comprehensive framework for the spatiotemporal statistical analysis of longitudinal shape data," International journal of computer vision, vol.103, no.1, pp.22–59, May 2013.

[5] T. Mansi, S. Durrleman, B. Bernhardt, M. Sermesant, H. Delingette, I. Voigt, P. Lurz, A.M. Taylor, J. Blanc, Y. Boudjemline, X. Pennec, and N. Ayache, "A statistical model of right ventricle in tetralogy of fallot for prediction of remodelling and therapy planning," International Conference on Medical Image Computing and Computer-Assisted Intervention, London, UK, pp.214–221, Sept. 2009.

[6] M. De Craene, O. Camara, B.H. Bijnens, and A.F. Frangi, "Large diffeomorphic FFD registration for motion and strain quantification from 3d-us sequences," International Conference on Functional Imaging and Modeling of the Heart, Nice, France, vol.5528, pp.437–446, June 2009.

[7] B.C. Davis, P.T. Fletcher, E. Bullitt, and S. Joshi, "Population shape regression from random design data," 2007 IEEE 11th International Conference on Computer Vision, Rio de Janeiro, Brazil, pp.1–7, Oct. 2007.

[8] U. Grenander, A. Srivastava, and S. Saini, "A pattern-theoretic characterization of biological growth," IEEE Transactions on Medical Imaging, vol.26, no.5, pp.648–659, April 2007.

[9] A. Trouvé and F.-X. Vialard, "Shape splines and stochastic shape evolutions: A second order point of view," Quarterly of Applied Mathematics, vol.70, no.2, pp.219–251, Feb. 2012.

[10] S.B. Alam and S. Kobashi, "Space-time statistical shape model for temporal three-dimensional shape change analysis of the adult brain," the 35th JAMIT annual meeting, OP6–2, Chiba, Japan, July 2016.

[11] B. Schölkopf, A.J. Smola, and K.R. Müller, "Kernel principal component analysis," in Advances in kernel methods: support vector learning, ed. B. Schölkopf, C.J. Burges, and A.J. Smola, pp.327–352, MIT press, Massachusetts, 1999.

[12] R. Pless and R. Souvenir, "A survey of manifold learning for images," IPSJ Transactions on Computer Vision and Applications, vol.1, pp.83–94, March 2009.

[13] Lina, T. Takahashi, I. Ichiro, and H. Murase, "Construction of appearance manifold with embedded view-dependent covariance matrix for 3D object recognition," IEICE Transactions on Information and Systems, vol.E91-D, no.4, pp.1091–1100, April 2008.

[14] M. Yamada, H. Hontani, and H. Matsuzoe, "A study on model selection from the q-exponential distribution for constructing an organ point distribution model," Pacific-Rim Symposium on Image and Video Technology, Auckland, New Zealand, vol.9555, pp.258–269, Nov. 2015.

[15] T. Kameda, S. Yamada, C. Uwabe, and N. Suganuma, "Digitization of clinical and epidemiological data from the Kyoto Collection of Human Embryos: maternal risk factors and embryonic malformations," Congenital anomalies, vol.52, no.1, pp.48–54, Feb. 2012.

[16] R. O'Rahilly and F. Müller, Developmental Stages in Human Embryos, Carnegie Institution of Washington Publication, Washington DC, 1987.

[17] M. Osaka, A. Ishikawa, S. Yamada, C. Uwabe, H. Imai, T. Matsuda, A. Yoneyama, T. Takeda, and T. Takakuwa, "Positional changes of

the ocular organs during craniofacial development," The Anatomical Record, 2017, in press.

[18] V. Arsigny, P. Fillard, X. Pennec, and N. Ayache, "Log-Euclidean metrics for fast and simple calculus on diffusion tensors," Magnetic resonance in medicine, vol.56, no.2, pp.411–421, June 2006.

[19] A. Takatsu, "Wasserstein geometry of Gaussian measures," Osaka Journal of Mathematics, vol.48, no.4, pp.1005–1026, Dec. 2011.

[20] A. Ohara, N. Suda, and S. Amari, "Dualistic differential geometry of positive definite matrices and its applications to related problems," Linear Algebra and Its Applications, vol.247, pp.31–53, Nov. 1996.

[21] H. Shima, "Hessian structures and information geometry," in The Geometry of Hessian Structures, ed. H. Shima, pp.103–114, World Scientific Publishing, Hong Kong, 2007.

[22] C.M. Bishop, Pattern Recognition and Machine Learning, Springer, New York, 2006.

[23] H. Akaike, "A new look at the statistical model identification," IEEE transactions on automatic control, vol.19, no.6, pp.716–723, Jan. 1974.

[24] S. Kotz and S. Nadarajah, Multivariate t-Distributions and Their Applications, Cambridge University Press, Cambridge, 2004.

[25] K. Shiota, S. Yamada, T. Nakatsu-Komatsu, C. Uwabe, K. Kose, Y. Matsuda, T. Haishi, S. Mizuta, and T. Matsuda, "Visualization of human prenatal development by magnetic resonance imaging (MRI)," American Journal of Medical Genetics Part A, vol.143A, no.24, pp.3121–3126, Dec. 2007.

[26] M.A. Styner, K.T. Rajamani, L.-P. Nolte, G. Zsemlye, G. Székely, C.J. Taylor, and R.H. Davies, "Evaluation of 3D correspondence methods for model building," Biennial International Conference on Information Processing in Medical Imaging, Ambleside, UK, vol.2732, pp.63–75, Springer, July 2003.

[27] A. Saito, A. Shimizu, H. Watanabe, S. Yamamoto, S. Nawano, and H. Kobatake, "Statistical shape model of a liver for autopsy imaging," International journal of computer assisted radiology and surgery, vol.9, no.2, pp.269–281, March 2014.

Masashi Kishimoto received the B.E. and M.E. degrees from Tokyo University of Agriculture and Technology in 2015 and 2017, respectively. Presently, with Mizuho Information & Research Institute, Inc., Japan.

Atsushi Saito received the B.E., M.E. and Ph.D. degrees from Tokyo University of Agriculture and Technology in 2011, 2013 and 2016, respectively. From 2015 to 2016, He was a research fellow of the Japan Society for the Promotion of Science. Since 2016, he has been an assistant professor at Tokyo University of Agriculture and Technology. His research activities are in the areas of image processing, pattern recognition and their applications to medical image analysis. He is the member of the Japanese Society of Medical Imaging Technology.

Tetsuya Takakuwa MD, graduated from University of Tokyo, Faculty of Science in 1986, and graduated from Osaka University, Faculty of Medicine in 1990. He worked as an Acute Care Physician at Osaka University Hospital and Critical Care and Emergency center Iwate Medical collage for 8 years. During those years, he got an opportunity to study at Max-Plank Institute for Immuno-biology in Germany. He took the role of Associate professor Department of Pathology, Osaka University Graduate School of Medicine in 2002, and received his PhD in 2005. He has become Professor of Kyoto University Graduate School of Medicine, Department of Human Health Science since 2008.

Shigehito Yamada graduated from the Faculty of Medicine at Kyoto University in 1998 and started his career as a Medical Doctor of Obstetrics and Gynecology. He also started the research about human embryology in 1995 when he was a medical student, continued his work and then received his PhD in 2006 by the work about making tutorial software of clinical embryology at the Graduate School of Medicine, Kyoto University. He then took the role of Assistant Professor of Congenital Anomaly Research Center (CARC), Kyoto University Graduate School of Medicine and also became the Research Fellow at Laboratory of Developmental Biology, NHLBI/NIH in 2006. He has become the associate professor of CARC since 2008, and now he is the professor of CARC and a professor of Human Health Sciences, Kyoto University Graduate School of Medicine. He is a board certified doctor of the Japan Society of Obstetrics and Gynecology, and also of Japanese Board of Medical Genetics.

Hiroshi Matsuzoe graduated from the Graduate School of Information Sciences, Tohoku University, in 1999. During 1999 to 2004, he joined Saga University, where he was an assistant professor, lecturer and associate professor. Since 2005, he is with Nagoya Institute of Technology, where he is now a professor. His research activities are in the area of differential geometry and differential geometrical method of mathematical science. He is a member of the Mathematical Society of Japan. He holds B.S., M.S. and Ph.D. degrees.

Hidekata Hontani received the B.E. and M.E. degrees from the University of Tokyo in 1991 and 1993, respectively. From 1993 to 1996, he joined Toshiba Corp. From 1996 to 2000, he was a research associate at the University of Tokyo and he received a Ph.D. degree from the University of Tokyo in 2000. From 2000 to 2004, he was an associate professor at Yamagata University. Since 2005, he joined Nagoya Institute of Technology, where he is a professor. During 2010, he was a researcher at UCLA, U.S.A. His research activities include image processing, pattern recognition, and signal processing. He is the member of IEEE, SICE, and IEICE.
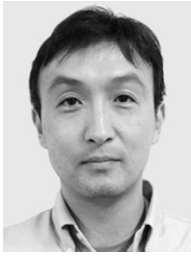
Akinobu Shimizu received the B.E., M.E. and Ph.D. degrees from Graduate School of Engineering, Nagoya University in 1989, 1991 and 1995, respectively. From 1994 to 1998, he was a research associate at Nagoya University. Since 1998, he joined Tokyo University of Agriculture and Technology, where he is a professor. His research activities are in the areas of image processing, pattern recognition and its application to medical image analysis. He is the member of the IEEE, the MICCAI, the CARS, the Information Processing Society in Japan, the Japanese Society for Medical and Biological Engineering and the Japanese Society of Medical Imaging Technology.